*Advances in Modern Agriculture* (2023) Volume 4 Issue 1
doi: 10.54517/ama.v4i1.2057

ORIGINAL RESEARCH ARTICLE

# Water droplet distribution for non-circular sprinkler nozzles

**Jialing Liu[1,2], Jixiang Wan[3], Hao Li[1,*], Yue Jiang[2]**

[1] *Chinese Academy of Agricultural Sciences, Farmland Irrigation Research Institute/Henan Province Water-saving Agriculture Key Laboratory, Xinxiang 453002, China*

[2] *Jiangsu University the Research Center for Fluid Mechanical Engineering Technology, Zhenjiang 212013, China*

[3] *Suqian Water Resources Bureau, Suqian 223999, China*

*** Corresponding author:** Hao Li, lihao01@caas.cn

## ABSTRACT

Objective: The study sought to investigate the distribution law of the diameter, velocity, and kinetic energy of water droplets in specially designed nozzles. Method: An indoor windless water droplet dispersion test on the PY15 rocker-arm sprinkler was performed using a video raindrop spectrometer at five working pressures: 100 kPa, 150 kPa, 200 kPa, 250 kPa, and 300 kPa. Result: The equal-flow nozzle has the following range: circle > rhombus > ellipse; the shape coefficient of the special-shaped nozzle decreases with increasing outlet diameter and increases with increasing aspect ratio; the diameter of the rhombus nozzle's water droplet increases radially. Conclusion: Under the same working pressure, the diameter of the water droplet at the end decreases as the form coefficient increases. The wider the outlet's diameter, the longer the range and the greater the increase in the velocity of the water droplets. The larger the aspect ratio, the shorter the range and the greater the average diameter and velocity of the droplets. The elliptical nozzle has the lowest droplet velocity increase as droplet diameter increases. The impacting kinetic energy and growth range of water droplets per unit volume at the same position decrease as the pressure increases. Along the radial direction, the droplet velocity and diameter are logarithmic, while the droplet kinetic energy and diameter are exponential and linear functions. The relationship between the shape coefficient, outlet diameter, aspect ratio, and droplet distribution characteristics of the shaped nozzle can be simulated using the fitting coefficients of the three droplet distribution prediction models, all of which are above 0.9.

***Keywords:*** rocker nozzle; shaped nozzle; video raindrop spectrometer; water droplet diameter distribution; droplet kinetic energy distribution

## 1. Introduction

Research significance: Sprinkler irrigation is an effective way of irrigation. An agricultural water-saving irrigation system generally consists of water engineering, water pumps and power equipment, a water pipe system, and the nozzle parts, such as the nozzle. The pros and cons of its performance not only directly affect the quality of spraying, but also relate to the entire economy[1–3].

Research progress: Sprinkler hydraulic performance mainly includes range, flow rate, working pressure, sprinkler irrigation intensity, sprinkler irrigation uniformity, water drop impact intensity, etc. Among them,

**ARTICLE INFO**
Received: 2 May 2023 | Accepted: 5 June 2023 | Available online: 12 June 2023

**CITATION**
Liu J, Wan J, Li H, Jiang Y. Water droplet distribution for non-circular sprinkler nozzles. *Advances in Modern Agriculture* 2023; 4(1): 2057. doi: 10.54517/ama.v4i1.2057

sprinkler irrigation intensity, sprinkler irrigation uniformity, and droplet impact intensity are related to the distribution characteristics of spray droplets. Therefore, the diameter of the spray droplets, the velocity of the droplets, and the kinetic energy of the droplets are important indicators to evaluate the quality of the sprinkler irrigation system, which have an important impact on the hydraulic performance of sprinkler irrigation[4–6].

The shape of the conventional nozzle is round. As a new type of non-circular nozzle, the special-shaped nozzle has the advantages of improving the water distribution of the nozzle, spraying uniformity, and better hydraulic performance under low pressure than the circular nozzle. It has been widely used in the field of agricultural sprinkler irrigation. A lot of research has been done on the distribution characteristics of spray droplets with various shapes of nozzles. Xu et al.[7] and Sanchez et al.[8] studied the distribution of droplet diameter and obtained the normal distribution model of droplet diameter, square root normal distribution model, log normal distribution model, and upper limit log normal distribution model (ULLN) in the spraying area. Gong[9], such as using a video raindrop spectrometer for a Nelson 3000 nozzle under different pressure drop diameter distributions along the range of research, analyzes the change trend of droplet diameter along the range and water droplet velocity, angle, and the relationship between water droplet diameter. The results show that the relationship between range accords with an exponential function and the diameter of water droplets, a logarithmic relation with the drop diameter droplet speed. Lorenzini[10] studied the law of droplet velocity and evaporation under different working pressures in the process of sprinkler irrigation and spraying. The results showed that air temperature had a significant impact on droplet evaporation, and air friction may be wrongly ignored when calculating droplet evaporation. Ouazaa et al.[11] used the ballistic model to study and analyze the velocity and kinetic energy of water droplets, and the results showed that under working pressures of 138 kPa and 69 kPa, the kinetic energy loss decreased with the increase in nozzle diameter. Zhu[12], such as the jet nozzle, is studied through experiments of a single water droplet’s kinetic energy, unit volume water droplet’s kinetic energy and kinetic energy intensity distribution, the kinetic energy intensity uniformity coefficient, and the relationship between the combination spacing. The results show that the jet nozzle’s kinetic energy distribution and a power function relation between drop diameter and unit volume water droplet’s kinetic energy increase along the radial is a function relationship. All the above studies are aimed at circular nozzles. Chen et al.[13] studied the influence of shape coefficients of four special-shaped nozzles, namely diamond, semicircle + triangle, semicircle + rectangle, and star, on droplet diameter and obtained the conclusion that the diameter of the terminal droplet decreases with the increase of shape coefficient. Li et al.[14] discussed the influence of the shape and pressure change of the irregular nozzle on the morphology change of the low-pressure jet and analyzed the influence of the change of the nozzle outlet shape, pressure, and inlet angle on the morphology change of the jet through experiments. Zhou et al.[15] designed a variety of special-shaped nozzles using the principle of the same area, discussed the sprinkler irrigation uniformity of special-shaped nozzles through experiments, and found that the combination uniformity coefficient of special-shaped nozzles was significantly higher than that of circular nozzles. Jiang et al.[16] used high-speed photography (HSP) technology to study the breaking process and flow characteristics of the shaped nozzle and found that the triangular jet has the shortest breaking length and the highest diffusion angle of the jet under the same pressure. The hydraulic performance of the profiled nozzle is improved under low pressure because the profiled nozzle produces different jet shapes. Compared with the circular nozzle, the range of the shaped nozzle is reduced, but the uniformity of sprinkler irrigation at low pressure is higher and the distribution of water droplets is more uniform.

Entry point: To sum up, because of its special geometric structure, the special-shaped nozzle has a variable jet shape, which can reduce the working pressure of the nozzle and improve its hydraulic performance. The quantitative study of the water droplet distribution characteristics of the profile-shaped nozzle under different working pressures will be helpful to promote the rational application of the profile-shaped nozzle.

Key issues to be solved: It is proposed to solve the key issues with abnormity nozzles as the research object, design three different shapes of nozzles using video raindrop spectrometer tests under different working conditions of different shapes of nozzle drop diameter distribution, droplet velocity distribution, and water droplet kinetic energy distribution, and explore the sprinkler hydraulic performance under the influence of the law of water distribution characteristics in order to further improve spraying performance. Select the appropriate pressure parameters of the special-shaped nozzle to provide a theoretical basis.

## 2. Materials and methods

### 2.1. Structural design of shaped nozzle

The size and design of the outlet section of the special-shaped nozzle can be determined according to the following two outlet methods: a. The principle of the same area, that is, the area number of the nozzle outlet section is the same. Take the outlet cross-sectional area of the circular nozzle as the standard to ensure that the outlet cross-sectional area of the irregular nozzle is equal to that of the circular nozzle. b. Principle of the same flow rate; that is, the flow rate through the nozzle is the same. Taking the outlet area of the circular nozzle as the standard, the area of the corresponding special-shaped nozzle is determined by the conversion of the formula $Q_P = 3600A\mu(2gH)^{1/2}$ to ensure that the flow rate of the special-shaped nozzle is consistent with that of the circular nozzle under the same working pressure.

Compared with the common circular nozzles, the elliptical and rhombic nozzles with equal flow rates were designed by adopting the principle of the same flow rate. The circular nozzle structure is shown in **Figure 1**. Where $d_0$ is the outlet diameter of the circular nozzle, which is 4 mm, 5 mm, and 6 mm; respectively; $\theta$ is the nozzle inlet cone angle, and 45 is selected; other structural parameters are the same. The outlet shapes and sizes of the nine nozzles studied in this paper are shown in **Table 1**.

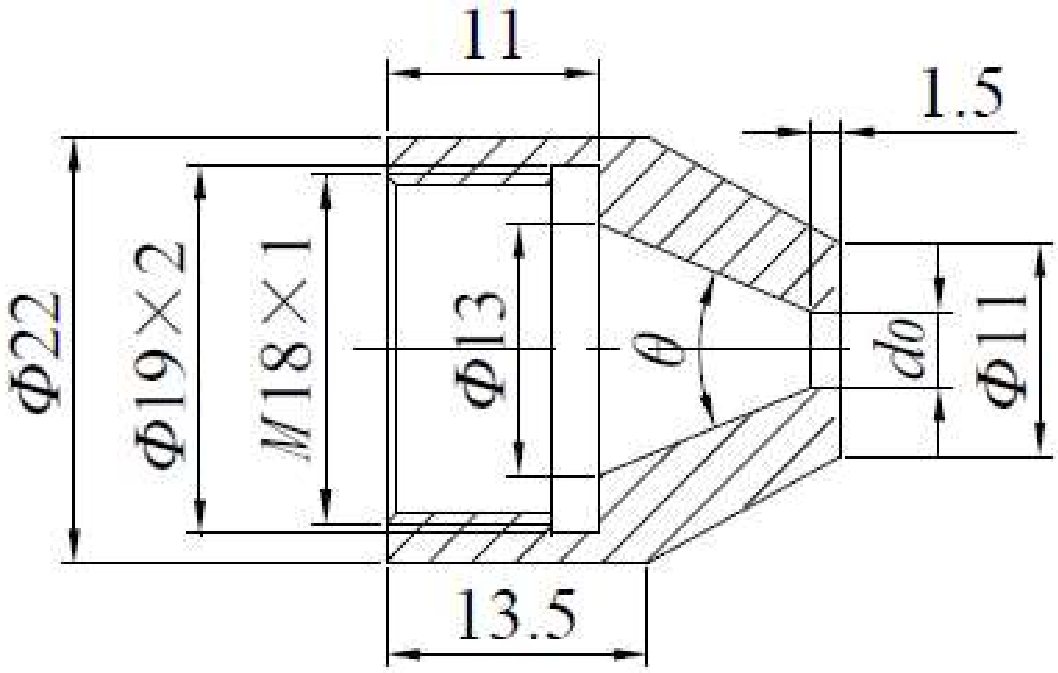


**Figure 1.** Diagram of nozzle structure.

**Table 1.** Geometric parameters of non-circular nozzle.

| Inlet cone angle | Shape | Number | Outlet diameter | Long axis | Brachyaxis | Draw ratio |
|---|---|---|---|---|---|---|
| 45° | Circular | C1 | C1 | 4 | / | / |
| | | C2 | C2 | 5 | / | / |
| | | C3 | C3 | 6 | / | / |
| | Diamond | D1 | D1 | 4 | 6 | 3.9 |
| | | D2 | D2 | 5 | 7 | 5.3 |
| | | D3 | D3 | 6 | 8 | 7.2 |
| | Ellipse | E1 | E1 | 5 | 6 | 4.2 |
| | | E2 | E2 | 5 | 7 | 3.5 |
| | | E3 | E3 | 5 | 8 | 3.1 |

The material of each nozzle processed by wire cutting is aluminum. Considering the error, the flow error test was carried out after machining, and it was found that the flow error of the special-shaped nozzle with the same inlet cone angle and outlet diameter was less than 4% under the same pressure (**Table 2**), so it was considered to be in line with the principle of the same flow rate.

**Table 2.** Equal flow nozzle flow error table in different pressures.

| Outlet diameter /mm | Number | Operating pressure/kPa | | | | | |
|---|---|---|---|---|---|---|---|
| | | 150 | 200 | 250 | 300 | 350 | 400 |
| 5 | C2 | 1.067 | 1.234 | 1.385 | 1.516 | 1.636 | 1.747 |
| | D2 | 1.036 | 1.198 | 1.347 | 1.476 | 1.601 | 1.709 |
| | Error/% | 2.91 | 2.92 | 2.74 | 2.64 | 2.14 | 2.18 |
| | E2 | 1.075 | 1.261 | 1.411 | 1.554 | 1.673 | 1.79 |
| | Error/% | 0.75 | 2.19 | 1.88 | 2.51 | 2.26 | 2.46 |
| | E3 | 1.064 | 1.237 | 1.386 | 1.523 | 1.642 | 1.755 |
| | Error/% | 0.28 | 0.24 | 0.07 | 0.46 | 0.37 | 0.46 |
| | E1 | 1.035 | 1.207 | 1.353 | 1.485 | 1.604 | 1.715 |
| | Error/% | 3.00 | 2.19 | 2.31 | 2.04 | 1.96 | 1.83 |
| 4 | C1 | 0.693 | 0.81 | 0.898 | 0.981 | 1.067 | 1.142 |
| | D1 | 0.675 | 0.78 | 0.88 | 0.975 | 1.052 | 1.131 |
| | Error/% | 2.60 | 3.70 | 2.00 | 0.61 | 1.41 | 0.96 |
| 3 | C3 | 1.461 | 1.694 | 1.895 | 2.079 | 2.247 | 2.401 |
| | D3 | 1.487 | 1.726 | 1.926 | 2.118 | 2.288 | 2.453 |
| | Error/% | 1.78 | 1.89 | 1.64 | 1.88 | 1.82 | 2.17 |

**Figure 2** shows the nozzle physical map.

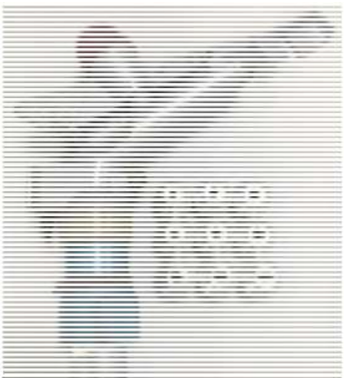

**Figure 2.** Nozzle physical map.

### 2.2. Test methods

The experiment of PY15 rocker sprinkler water distribution and droplet kinetic energy distribution was carried out in the indoor windless sprinkler irrigation experimental hall with a diameter of 44 m. The installation height of the nozzle is 1.4 m, and the working pressures are set to 100 kPa, 150 kPa, 200 kPa, 250 kPa, and 250 kPa respectively. Because there is no wind in the sprinkler irrigation hall, data on one ray can be used instead of all rays in the circle. The video raindrop spectrometer (developed by the European Space Agency and the European Space and Technology Centre and purchased by Ecotech Co., Ltd.) moved at a distance of 2 m after the nozzle operated stably for 10 min, and the diameter and speed of water droplets at each point were measured in turn. The testing time of the raindrop spectrometer at each point was that the nozzle rotated past the raindrop spectrometer three times. See **Figures 3** and **4** for the test system layout and field photos.

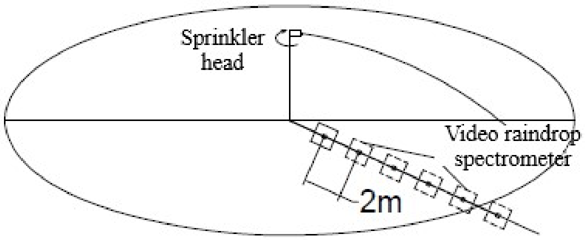


**Figure 3.** Schematic layout of the test system.

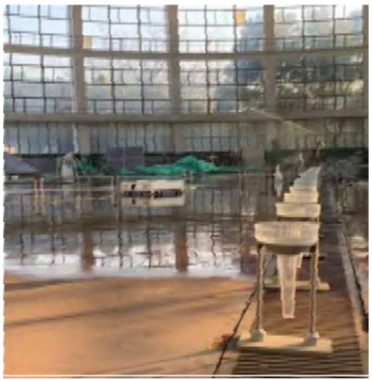

**Figure 4.** Test site photos.

### 2.3. Data processing methods

#### 2.3.1. Form factor

The diameter of water droplets increases with the distance from the nozzle, reaching the maximum at the end of the range[7]. Therefore, the diameter of the terminal water droplets can be used as an important basis to measure the atomization condition of the nozzle.

The influence of nozzle shape on water droplet diameter is generally expressed by shape coefficient. The more the nozzle shape deviates from the circle, the larger the shape coefficient $\beta$ is, and the greater the influence of nozzle shape on water droplet diameter. The relation of $\beta$ is shown in Equation (1):

$$\beta = \frac{X^2}{16A} \tag{1}$$

where: $X$ *is* the perimeter of the nozzle water-passing section (mm); $A$ is the cross-sectional area of nozzle water ($mm^2$).

### 2.3.2. Average diameter of water-weighted water droplets

The commonly used methods for calculating the diameter of water droplets at home and abroad include number weighting method, water weight weighted average method and median diameter method[17]. In this paper, the weighted average method of water weight is used to calculate the average diameter of water droplets at each measuring point. Exp2PMod1 index is fitted by origin, and the Equation (2) is:

$$d = ae^{bl} \tag{2}$$

where: $a$ and $b$ are fitting coefficients; $d$ is the diameter of water droplets; $l$ is the distance from the initial position of the nozzle.

### 2.3.3. Distribution law of water droplet diameter and velocity

The velocity of water droplets is an important factor to determine the kinetic energy of water droplets. The velocity of water droplets with different diameters from different nozzles is measured by video raindrop spectrometer.

There is a logarithmic function relationship between the diameter and velocity of water droplets, and the relationship Equation (3) is:

$$v = a - b\ln(d + c)^{[17]} \tag{3}$$

where: $a$, $b$ and $c$ are the fitting coefficients; $v$ is the speed of water droplets; $d$ is the diameter of water droplets.

### 2.3.4. Kinetic energy of water droplets per unit volume[15]

The kinetic energy of water droplets per unit volume refers to the ratio of the total kinetic energy of individual water droplets at different measuring points to the total volume, and the relation is shown in Equation (4):

$$E_{\text{ks}} = \frac{\sum_{j=1}^{m} E_{\text{sd}_j}}{1000\sum_{j=1}^{m} \frac{1}{6}\pi \cdot W \cdot d_j^3} \tag{4}$$

where $E_{\text{ks}}$ is the kinetic energy of water droplets per unit volume (J/L); $j$ is the name of water droplet diameter level; $m$ is the particle diameter series.

## 3. Results and analysis

### 3.1. Shape coefficient and end drop diameter

**Table 3** shows the range of the PY15 nozzle under different pressures. It can be seen from **Table 3** that for constant flow nozzles C2, D2, E1, E2, and E3, the range of a circular nozzle is greater than the range of a diamond nozzle, and the range of an elliptical nozzle is greater. The larger the diameter of the outlet, the farther the range; the larger the aspect ratio, the closer the range.

**Table 3.** Range of PY15 nozzle under different pressures.

| Nozzle shape | Number | Operating pressure/kPa | | | | |
|---|---|---|---|---|---|---|
| | | 100 | 150 | 200 | 250 | 300 |
| Circular | C2 | 11 | 14 | 14 | / | / |
| | D1 | 11 | 12 | 13 | 13 | 13 |
| Diamond | D2 | 10 | 12 | 13 | 14 | 14 |
| | D3 | 11 | 13 | 14 | / | / |
| | E1 | 9 | 11 | 12 | 13 | 14 |
| Ellipse | E2 | 10 | 11 | 12 | 12 | 13 |
| | E3 | 9 | 10 | 11 | 11 | 12 |

**Table 4** shows the diameter of terminal water droplets under low pressure of 100 kPa, 150 kPa, and standard pressure of 200 kPa. The shape coefficient decreases with the increase of the outlet diameter, where: x is the circumference of the nozzle's cross section (mm); A is the cross-sectional area of nozzle water ($mm^2$). It increases with the increase in length-diameter ratio. The greater the working pressure, the smaller the diameter of the end water drop. The larger the shape coefficient, the smaller the diameter of the terminal water drop under the same working pressure. For constant flow nozzles C2, D2, E1, E2, and E3, under low pressures of 100 kPa and 150 kPa, the diameter of water droplets at the ends of elliptical nozzles with different aspect ratios is the smallest, while that of circular nozzles is the largest. With the increase in pressure to 200 kPa, the diameter of water droplets at the end of the diamond nozzle is the largest, while that of the round nozzle decreases the fastest with the increase in pressure. As can be seen from **Tables 3** and **4**, among the constant flow nozzles at low pressure, the elliptical nozzle has the smallest range and the smallest diameter of water droplets at the end. The range of the circular nozzle is the longest, and the diameter of the water droplets at the end is the largest at low pressures of 100 kPa and 150 kPa and the smallest at 200 kPa. The range of the diamond nozzle is moderate, and the diameter of the water droplets at the end is the largest at 200 kPa.

**Table 4.** Shape coefficient and diameter of end water drops of non-circular nozzle.

| Nozzle shape | Number | Form factor | Operating pressure/kPa | | |
|---|---|---|---|---|---|
| | | | 100 | 150 | 200 |
| Circular | C2 | 0.785 | 6.545 | 5.388 | 3.691 |
| Diamond | D1 | 1.094 | 5.811 | 4.373 | 4.039 |
| | D2 | 1.039 | 5.659 | 4.791 | 4.502 |
| | D3 | 1.006 | 7.020 | 5.195 | 4.588 |
| Ellipse | E1 | 0.890 | 3.226 | 4.353 | 3.915 |
| | E2 | 1.052 | 4.737 | 3.984 | 3.964 |
| | E3 | 1.225 | 4.129 | 3.328 | 1.952 |

## 3.2. Diameter distribution of water droplets

### 3.2.1. Radial distribution of droplet diameter under different pressures

By fitting the measured data, it can be found that the fitting correlation coefficient R2 of nozzles of all shapes under each working pressure is greater than 0.9, indicating that the fitting accuracy of this exponential function is high.

**Figure 5** shows the relationship between the average diameter and distance of water droplets under different working pressures. As can be seen from **Figure 5**, for the nozzle with the same shape, the higher the pressure, the smaller the slope of the exponential function curve, and the smaller the average diameter of the water droplets at the same measuring point. This indicates that the increase in pressure makes the diameter of the water droplets decrease along the trend of increasing the distance from the initial position of the nozzle and the more intense the degree of jet fragmentation. The slope of the C2 curve of the circular nozzle decreases the most. In addition, under the same pressure, among the three nozzles with different shapes, the curve slope of the diamond-shaped nozzle is the largest, while that of the circular nozzle is the smallest, which indicates that the droplet diameter of the diamond-shaped nozzle increases the most along the distance from the initial position of the nozzle.

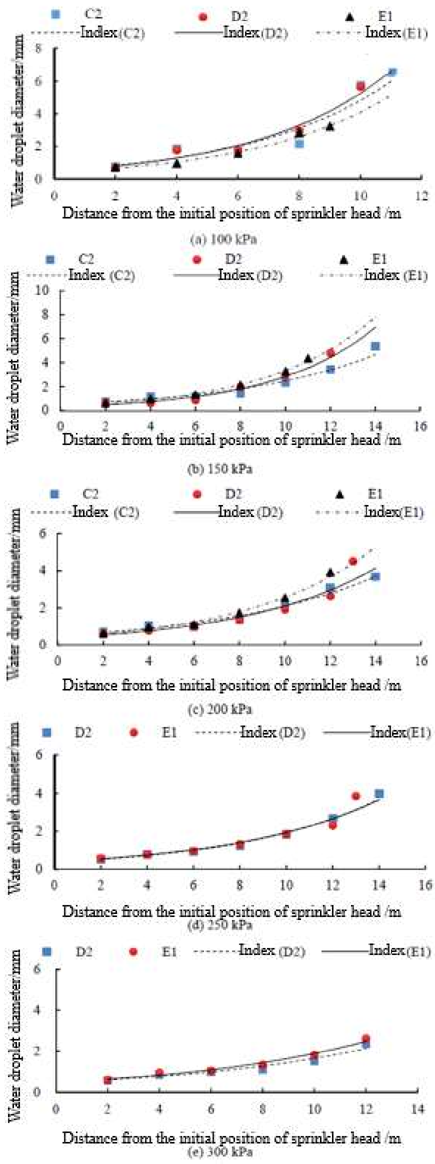


**Figure 5.** Relationship curve of mean diameter and distance of water drops under different pressures.

In addition, when the droplet diameter was 3 mm, the distance between the circular nozzle C2 and the initial position of the nozzle at 100 kPa, 150 kPa, and 200 kPa was 7.9 m, 11 m, and 12.4 m, respectively. The distance between the rhomboid nozzle D2 and the initial position of the nozzle at 100 kPa, 150 kPa, 200 kPa, and 250 kPa was 7.6 m, 10 m, 11.7 m, and 12.5 m, respectively. The distance from the initial position of the elliptical nozzle E1 at 100 kPa, 150 kPa, 200 kPa, and 250 kPa was 8.5 m, 9.5 m, 10.7 m, and 12.3 m, respectively. The droplet diameter of the diamond and oval nozzles at 300 kPa is less than 3 mm. Since water droplets with a small diameter are prone to drift and evaporation loss, and water droplets with a large diameter are also damaging to soil surface structure, which is not conducive to soil and water conservation and crop growth, the diameter range of water droplets suitable for spraying is 1–3 mm. Therefore, it can be seen that the suitable spraying range is the largest except for the oval nozzle E1 at 100 kPa. Under other working pressures, the suitable spraying range of circular nozzle C2 is the largest. When the distance is greater than 8 m, the pressure has an obvious effect on the droplet diameter.

### 3.2.2. Radial distribution of droplet diameter with different aspect ratio

For the nozzle with the same aspect ratio, the slope of the droplet diameter exponential function decreases with the increase in pressure; that is, the increase in pressure decreases the tendency of the droplet diameter to increase along the radial direction. Under the same pressure and with different aspect ratios of the same shape, inlet cone angle, and outlet diameter, the droplet diameters at each measuring point are almost the same within 6 m from the initial position of the nozzle. The relation of the average diameter of water droplets along the radial direction generally satisfies the rule of E3 > E2 > E1, that is, the larger the aspect ratio, the larger the average diameter of water droplets. The nozzle E3 with the largest aspect ratio has the shortest range and the largest droplet diameter overall. The nozzle E1 with the smallest aspect ratio has the smallest diameter of water droplets along the radial direction and has a relatively long range. Therefore, a nozzle with a smaller length and diameter can be selected for sprinkler spraying. **Figures 6** and **7** show the relationship curve of mean diameter and distance of water drops at different length-dimension ratio and relationship curve of mean diameter and distance of water drops at different outlet diameters, respectively.

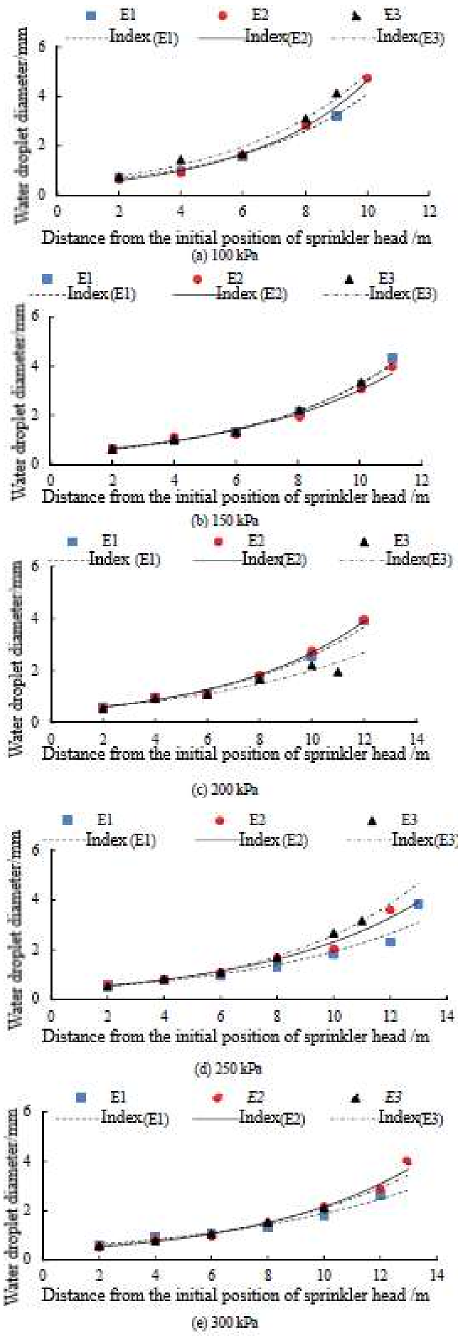


**Figure 6.** Relationship curve of mean diameter and distance of water drops at different length-dimension ratio.

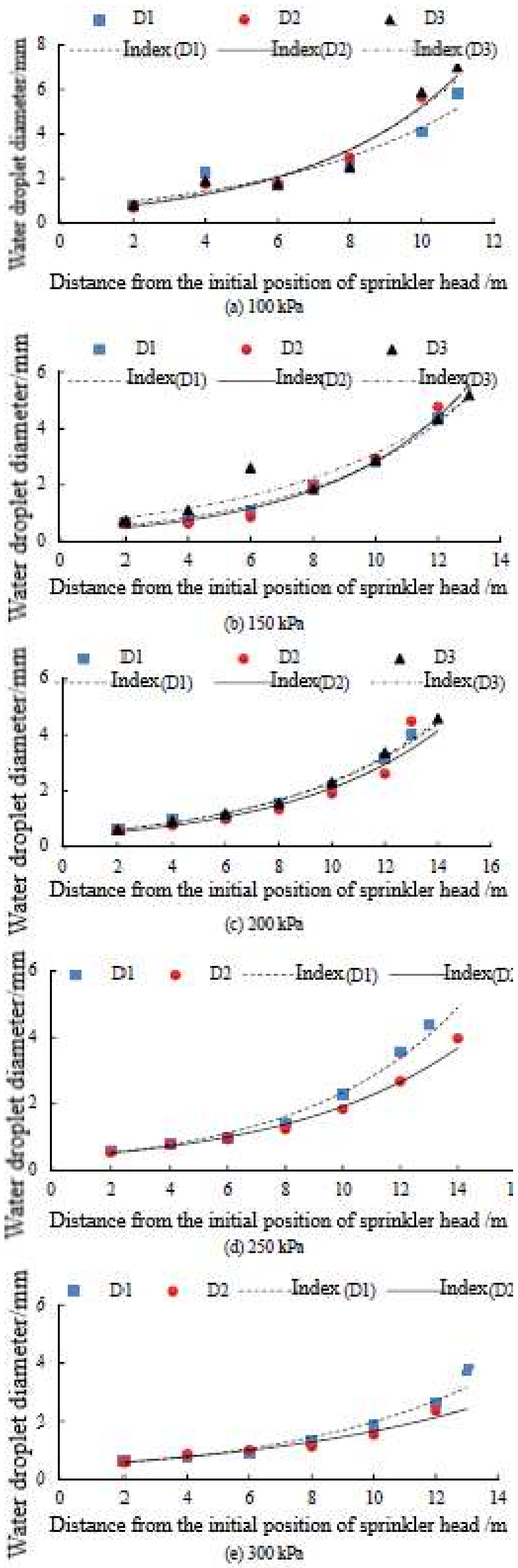


**Figure 7.** Relationship curve of mean diameter and distance of water drops at different outlet diameters.

### 3.2.3. Radial distribution of nozzle droplet diameter with different outlet diameters

The inlet cone angles of rhomboid nozzles D1, D2, and D3 are 45°, and the outlet diameters are 4 mm, 5 mm, and 6 mm, respectively. The average diameter of water droplets and the slope of the curve generally meet the relationship of D3 > D1 > D2, that is, the outlet diameter is 6 mm > 4 mm > 5 mm. The average droplet diameter of the nozzle with the largest outlet diameter, D3, is the largest, while the average droplet diameter of the nozzle with the outlet diameter of 5 mm is the smallest. With the increase in pressure, the slope of the curve decreases; that is, the droplet diameter decreases along the longitudinal growth amplitude, and the drop diameter of the nozzle with the outlet diameter of 5 mm decreases the largest. Therefore, a nozzle with an outlet diameter of 5 mm can be selected for sprinkler spraying.

### 3.3. Water drop velocity distribution

#### 3.3.1. Drop velocity distribution of nozzles with different shapes

**Figure 8** shows the relationship between the average diameter and velocity of droplets from nozzles with different shapes. It can be seen from **Figure 8** that for nozzles with the same inlet cone angle and outlet diameter, the slope of the velocity curve of the circular nozzles is the largest, while that of the elliptical nozzles is the smallest. That is, with the increase in droplet diameter, the droplet velocity of the elliptical nozzles increases the least. The droplet velocity increases with the increase in droplet diameter, which gradually decreases, indicating that droplet diameter is an important factor affecting droplet velocity. In general, the fitted curves of droplet velocity and droplet diameter of the three special-shaped nozzles with equal flow rate are almost exactly the same, indicating that under the premise of the same flow rate, inlet cone angle, and outlet diameter, the nozzle outlet shape has little influence on the relationship between average droplet diameter and velocity.

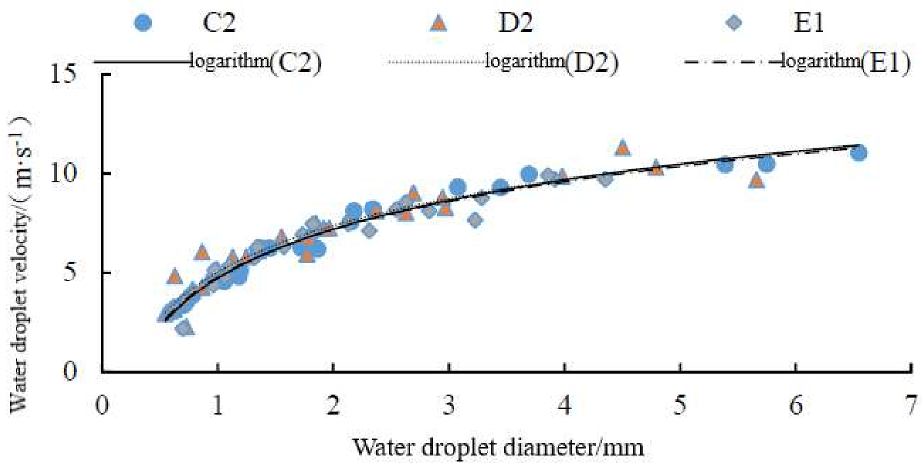


**Figure 8.** Relationship curve of average diameter and velocity of water drops in different shapes.

#### 3.3.2. Droplet velocity distribution with different aspect ratio

The relationship between droplet diameter and velocity of elliptical nozzles with different aspect ratios is shown in **Figure 9**. It can be seen from **Figure 9** that for elliptical nozzles with the same inlet cone angle and outlet diameter but different aspect ratios, the slope of the velocity curve is E3 > E2 > E1, that is, the slope of the velocity curve increases with the increase of aspect ratio, and the increase of aspect ratio makes the drop velocity increase with the increase of droplet diameter. At the same droplet diameter, the droplet velocity of nozzle E2 is always the maximum. In the range of droplet diameter less than 2.5 mm, the droplet velocity of the elliptic nozzle satisfies E1 > E3. When the droplet diameter is larger than 2.5 mm, the droplet velocity is E3 > E1. This indicates that there is an intermediate aspect ratio between the maximum and minimum aspect ratios. Under this aspect ratio, the droplet velocity is the largest when the droplet diameter is the same, as is the kinetic energy of droplet impact.

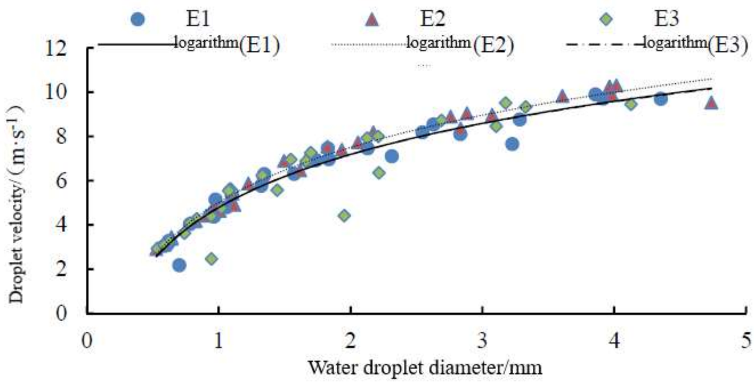


**Figure 9.** Relationship curve of average diameter and velocity of water drops with different length-dimension ratio.

### 3.3.3. Drop velocity distribution with different outlet diameters

The relationship between droplet diameter and velocity of rhomboid nozzles with different outlet diameters is shown in **Figure 10**. It can be seen from **Figure 10** that for nozzles with the same shape and inlet cone angle, the slope of the velocity curve is shown as D3 > D2 > D1, that is, the slope of the curve increases with the increase in outlet diameter. The larger the outlet diameter, the larger the drop velocity increases with the increase in drop diameter. When the droplet diameter is less than 5 mm, it is D1 > D2 > D3, indicating that the larger the outlet diameter is, the smaller the droplet velocity is.

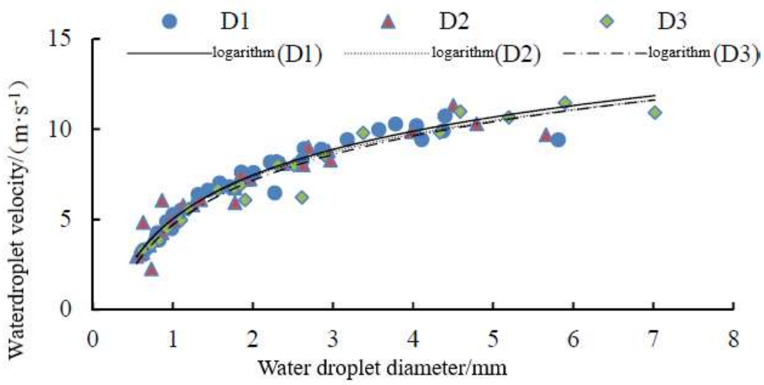


**Figure 10.** Relationship curve of water drop velocity and distance of different outlet diameter nozzle.

## 3.4. Distribution law of hitting kinetic energy of droplets per unit volume

**Figure 11** shows the radial distribution of kinetic energy per unit of water drop under different pressures. The larger the pressure, the smaller the kinetic energy of the droplets per unit volume at the same position, the smaller the growth range of kinetic energy, and the smaller the damage to crops and soil. At a close distance of 2 m, there is little difference in the kinetic energy of droplets per unit volume of each nozzle under each working pressure. It can be seen from **Figures 11(a)–11(c)** that the elliptical nozzle has the smallest hitting kinetic energy per unit volume of water droplets in the constant flow nozzles with the same inlet cone angle and outlet diameter at each working pressure. At 100 kPa, the maximum kinetic energy of droplets per unit volume of a circular nozzle is the largest. According to **Figures 11(c)–11(e)**, the larger the aspect ratio, the shorter the range. The elliptical nozzle E1 with the smallest aspect ratio at 100 kPa has the smallest drop-hitting kinetic energy per unit volume. Under 150–300 kPa, the nozzle E3 with the largest aspect ratio has the smallest kinetic energy of droplets per unit volume. According to **Figures 11(b)**, **11(f),** and **11(g)**, the smaller the outlet diameter, the smaller the kinetic energy of droplets per unit volume under 100–200 kPa.

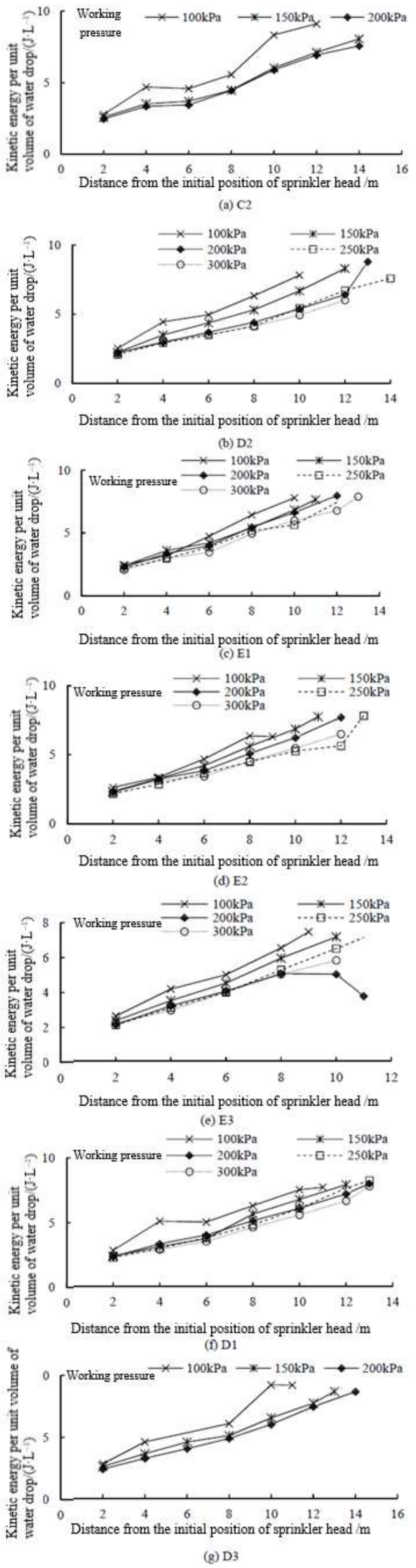


**Figure 11.** Graph of kinetic energy of water drop per unit body under different working pressures.

In order to further study the radial distribution law of droplet kinetic energy per unit volume of the profile-shaped nozzle, this paper established the distribution model of droplet kinetic energy and distance from the nozzle by regression analysis of droplet kinetic energy per unit volume of each nozzle under various pressures[13] (Equation (5)):

$$E_{\mathrm{ks}} = al + b \tag{5}$$

where: *a* and *b* are the fitting coefficients; $E_{\mathrm{ks}}$ is the kinetic energy of water droplets per unit volume, and *l* is the distance from the initial position of the nozzle.

The fitting coefficients of kinetic energy of water droplets per unit volume of a special-shaped nozzle are all above 0.9, and the fitting accuracy is high.

There will be three different length-to-diameter ratios of the oval nozzle under different working pressures per unit volume of water droplets. The kinetic data regression, the kinetic energy per unit volume further analysis, and the establishment of a special nozzle for spray droplets will determine the will determine the kinetic energy per unit volume. $E_{\mathrm{ks}}$, away from the nozzle distance *l*, length to diameter ratio mathematical model of the relationship between beta and working pressure *P*, function Equation (6) is:

$$E_{\mathrm{ks}} = 2.775P^{-0.318}l + 0.0926\beta + 0.932 \qquad (R^2 = 0.924) \tag{6}$$

where: *a* and *b* are the fitting coefficients; $E_{\mathrm{ks}}$ is kinetic energy of water droplets per unit volume; *l* is the distance from the initial position of the nozzle.

The fitting coefficient of kinetic energy of droplets per unit volume of elliptical nozzles with different aspect ratios is 0.924, which indicates that the fitting accuracy is high.

# 4. Discussion

Most of the existing studies on the distribution characteristics of water droplets in profile-shaped nozzles are focused on the influence of shape and pressure change on the change of jet morphology[13–16]. This study uses a video raindrop spectrometer to further study the influence of the shape and pressure of a profile-shaped nozzle on the distribution characteristics of water droplets, such as diameter, velocity, and kinetic energy. The results show that the shape coefficient of the special-shaped nozzle decreases with the increase of the outlet diameter, and the range increases with the increase of the outlet diameter. The larger the shape coefficient is, the smaller the diameter of the end droplet under the same working pressure is, which is consistent with the experimental conclusion of Chen et al.[13] on the shape coefficient of the special-shaped nozzle. The tendency of the droplet diameter to increase along the radial direction decreases with an increase in pressure. The larger the outlet diameter, the larger the droplet velocity increases with the droplet diameter. When the droplet diameter is the same, the larger the outlet diameter, the smaller the droplet velocity. The hitting kinetic energy and its growth amplitude of water drop per unit volume at the same position decrease with the increase in pressure. It is close to the conclusion of the study of Zhu et al.[12] on the spraying law of a full jet nozzle.

In addition, the effects of the aspect ratio of the profiled nozzle on the hydraulic performance and the water droplet distribution characteristics were also studied. The shape coefficient of the shaped nozzle increases with the increase in aspect ratio, and the range decreases with the increase in aspect ratio. Under five kinds of working pressure, the diameter of the water drop in the rhomboid nozzle increases the most along the radial direction. The larger the aspect ratio, the larger the droplet velocity increases with the droplet diameter. With the increase in droplet diameter, the growth range of droplet velocity in an elliptical nozzle is the smallest, while that of a circular nozzle is the largest. The average drop diameter of the nozzle with an outlet diameter of 5 mm is the smallest, and the drop diameter decreases the most along the longitudinal growth.

## 5. Conclusion

1) Using video raindrop spectrometer measuring technology of special-shaped nozzle spray drop diameter, velocity, and kinetic energy distribution of the test, and establish accurately reflect special nozzle spray droplets diameter, water speed, and water droplets kinetic energy per unit volume distribution prediction model of five kinds of working under pressure, seven special nozzle model fitting correlation coefficient is above 0.9. The larger the aspect ratio of the nozzle, the smaller the kinetic energy of droplets per unit volume. Among the nozzles with constant flow under each working pressure, the elliptical nozzles have the smallest kinetic energy of droplets per unit volume.

2) Under the working pressure of 100 kPa, 150 kPa, 200 kPa, 250 kPa, or 300 kPa, the larger the length-diameter ratio of the profile-shaped nozzle, the larger the average diameter of the water droplets. Under the same working pressure and different aspect ratio of the elliptical nozzles with constant flow, the droplet diameter at each measuring point is almost the same within 6 m from the initial position of the nozzle.

## Conflict of interest

The authors declare no conflict of interest.

## References


1. Bao Y, Liu J, Liu X, et al. Experimental study on effects of pressure on water distribution model of low-pressure sprinkler (Chinese). *Journal of Drainage and Irrigation Machinery Engineering* 2016; 34(1): 81–85.
2. Li J, Xu Z. Research on water-saving irrigation in the development of facility horticulture: Review of “water-saving irrigation technology” (Chinese). *Journal of Irrigation and Drainage* 2020; 39(1): 146.
3. Zhu X, Shi Y, Hu G, et al. Dynamic simulation and test of water distribution of fluidic sprinkler (Chinese). *Journal of Irrigation and Drainage* 2020; 39(4): 74–83.
4. Yuan S, Li H, Wang X. Status, problems, trends and suggestions for water-saving irrigation equipment in China (Chinese). *Journal of Drainage and Irrigation Machinery Engineering* 2015; 33(1): 78–92.
5. Wu P, Zhu D, Lv H, et al. *Introduction to Irrigation Hydraulics* (Chinese). Chinese Science Publishing & Media Ltd.; 2012.
6. Tu Q, Li H, Wang X, et al. Comparison and selection of small-scale irrigation machines with multiple sprinklers based on grey relational analysis (Chinese). *Journal of Jiangsu University (Natural Science Edition)* 2014; 35(6): 656–662.
7. Xu H, Gong S, Jia R, Liu X. Study on droplet size distribution of ZY sprinkler head (Chinese). *Journal of Hydraulic Engineering* 2010; 41(12): 1416–1422.
8. Sánchez Burillo G, Delirhasannia R, Playán E, et al. Initial drop velocity in a fixed spray plate sprinkler. *Journal of Irrigation and Drainage Engineering* 2013; 139(7): 521–531.
9. Gong X, Zhu D, Zhang L, et al. Drop size distribution of fixed spray-plate sprinklers with two-dimensional video disdrometer (Chinese). *Transactions of the Chinese Society for Agricultural Machinery* 2014; 45(8): 128–133+148.
10. Lorenzini G. Water droplet dynamics and evaporation in an irrigation spray. *Transactions of the ASABE* 2006; 49(2): 545–549.
11. Ouazaa S, Burguete J, Paniagua MP, et al. Simulating water distribution patterns for fixed spray plate sprinkler using the ballistic theory. *Spanish Journal of Agricultural Research* 2014; 12(3): 850. doi: 10.5424/sjar/2014123-5507
12. Zhu X, Liu X, Liu J, et al. Droplet kinetic energy distribution regulation of complete fluidic sprinkler (Chinese). *Transactions of the Chinese Society of Agricultural Engineering* 2015; 31(15): 26–31.
13. Chen C, Yuan S, Li H, Wang C. Effect of non-circle nozzle on hydraulic performance of impact variable-rate sprinkler (Chinese). *Transactions of the Chinese Society for Agricultural Machinery* 2011; 42(12): 111–115.
14. Li D, Lu X, Zhao X. Experimental study on low pressure jet characteristic of the non-circle jet nozzle (Chinese). *Light Industry Machinery* 2006; 24(3): 18–20.
15. Zhou X, Li H, Jiang Y. Study on water distribution uniformity of non-circular nozzles at low pressure (Chinese). *Journal of Drainage and Irrigation Machinery Engineering* 2017; 35(5): 448–453.
16. Jiang Y, Li H, Hua L, et al. Experimental study on jet breakup morphologies and jet characteristic parameters of non-circular nozzles under low-intermediate pressures. *Applied Engineering in Agriculture* 2019; 35(4): 617–632. doi: 10.13031/aea.13291

17. Wu P, Zhu D, Lv H, Zhang L. Hydraulics problems in farmland irrigation (Chinese). *Journal of Drainage and Irrigation Machinery Engineering* 2012; 30(6): 726–732.